AN EQUATION OF STATE OF CO FOR USE IN PLANETARY MODELING

M. Podolak

Dept. of Geosciences, Tel Aviv University, Tel Aviv, 69978 Israel

A. Levi

Braude College of Engineering, Karmiel, 2161002 Israel

A. Vazan

Astrophysics Research Center (ARCO), Dept. of Natural Sciences, Open University of Israel, Raanana, 43107 Israel

U. Malamud

Dept. of Geosciences, Tel Aviv University, Tel Aviv, 69978 Israel
Department of Physics, Technion – Israel Institute of Technology, Technion City, 3200003 Haifa, Israel

ABSTRACT

Although carbon monoxide (CO) is an abundant molecule and may have great importance for planetary interiors, measurements of its properties are difficult due to its extreme volatility. We calculate the equation of state for CO over a range of temperature and density that is applicable to the conditions in planetary interiors. Previous experimental and theoretical studies cover only a limited temperature-density range. Our calculations match these early results well, but now cover the full range of relevance. The method of calculation is based on the general-purpose quotidian equation of state described by More et al. (1988), which is here used in order to generate a freely downloadable look-up table to be used by the community.

1. INTRODUCTION

When modeling planetary interiors, it is necessary to have adequate descriptions for the behavior of the constituent materials. Thus equation of state (EOS) tables have been produced for the two most abundant elements in the universe, hydrogen and helium (see, e.g. Chabrier et al. 2019), as well as other materials expected to be of importance for planet models, such as water (see, e.g. Haldemann et al. 2020), various silicates such as dunite (Benz et al. 1989), granite (Pierazzo et al. 1997), basalt (Pierazzo et al. 2005), quartz (Melosh 2007) and important metals such as iron (e.g. Emsenhuber et al. 2018).

Since both carbon and oxygen have relatively high cosmic abundances, and since CO is a very stable molecule, CO could be an important constituent in planetary interiors (see, e.g. Lisse et al. 2022). Yet this possibility cannot be properly addressed because only limited regions of the CO EOS have been studied, and there are no complete equation of state tables available in the literature. Empirical measurements of the density of solid (α-cubic, β-hexagonal) and liquid CO have been made (Boon et al. 1967; Bierhals 2001), in addition to various other physical properties such as viscosity, heat capacity (Rudesko & Schubnikow 1934; Tancredi et al. 1994), and elastic constants (Gammon 1978). All of these studies are applicable to extremely low temperature and pressure conditions, and are ill-suited for planetary interior applications. The behavior of CO at higher pressures and temperatures has been studied, to a limited extent by Nellis et al. (1981) who reported the results of shock experiments. More recent work by Zhang et al. (2011) gives a more refined hugoniot for CO. In addition, theoretical calculations by Goodwin (1985) have investigated the region of pressures below 100 MPa. Individual pressure-temperature-density points have been computed from quantum molecular dynamics calculations by Massacrier et al. (2011), Wang & Zhang (2010), and Leonhardi & Militzer (2017). However, all of this data is insufficient for planetary modeling, where a much larger range of pressures and temperatures are encountered.

The fact that shock-derived carbon condensates have diameters of the order of a few nanometers (Titov et al. 1989; Viecelli et al. 2001; Krüger et al. 2005), and growth timescales of 100's of picoseconds (Armstrong et al. 2020)) make

amitlevi.planetphys@gmail.com

direct DFT based molecular dynamics simulations of this system particularly challenging. Overcoming such immense difficulties often requires some synthesis between a DFT based approach and more classical force field models using various training models often referred to as machine learning approaches (see, e.g. Lindsey et al. 2020; Singraber et al. 2019). These techniques are very demanding computationally. Therefore, our model which is in good agreement with experimental data and covers a very wide pressure-temperature domain is of merit.

To this end we have generated an equation of state table for CO which we describe below. Our calculation is admittedly more crude, but it should be sufficiently close to reality so as to be useful in establishing model trends such as was done in the models of Podolak et al. (2022), for example. This paper is structured as follows: Section 2 gives a brief description of the method for computing the quotidian EOS (QEOS). This computation requires the knowledge of the density and bulk modulus at low energy. The DFT calculation of these parameters is described in section 3, and the results are given in section 4. The resulting EOS table and its comparison to experimental and theoretical work described above is given in section 5. It is hoped that this work will encourage more detailed EOS modeling for CO in the future.

2. QUOTIDIAN EQUATION OF STATE

More et al. (1988) present a general-purpose method for computing equations of state at high pressure, called the Quotidian Equation of State (QEOS). The QEOS is a statistical-mechanics-based method, in which thermodynamic quantities are derived from the Helmholtz free energy. The Helmholtz free energy term is composed of three parts: an ionic contribution, an electronic contribution, and a bonding correction. The ionic part is calculated by the Cowan model, a semi-empirical model which interpolates between known limiting physical cases (ideal gas law, Lindemann melting law, Dulong-Petit law, Grüniesen EOS, Debye lattice). The electronic part is calculated using a modified Thomas-Fermi (TF) model. The TF model neglects attractive (bonding) forces between neutral atoms and therefore overestimates the critical point and the pressure near normal conditions. The bonding correction is used here to correct for the electronic part failure by calibration of the EOS with density and bulk modulus at reference conditions of zero (low) energy.

This method has been used to develop EOS tables for Fe, SiO_2 and H_2O for use in planetary modeling which compare well with other EOS tables such as SESAME and ANEOS for these substances (Vazan et al. 2013, 2018, 2022). The QEOS input variables are: atomic number, atomic weight, and reference conditions density and bulk modulus. The calculated quantities are: pressure, specific internal energy, and specific entropy. The temperature-density range of the calculation is $11.6 < T < 1.16 \times 10^6$ K, and $2.5 \times 10^{-13} < \rho < 100$ g cm^{-3}. The liquid-vapor phase transition is determined with regard to the Maxwell construction, based on finding equal Gibbs free energy on the liquid and the vapor sides of each isotherm (up to the critical temperature). As a result, there is no coexistence of vapor and liquid phases in the resulting smooth QEOS.

In order to calculate a QEOS for CO, the method requires prior knowledge of the density and bulk modulus of the material at very low temperature and pressure. Unfortunately there have been no measurements of these quantities for the α-phase of CO. We therefore performed a first-principles calculation for this state using density-functional theory (DFT). This calculation described in the next section.

3. COMPUTATIONAL METHODS

Here we study the equation of state of α-CO at 0 K. The structure is taken from Hall & James (1976). We performed static total energy relaxations with the CP2K code (Kühne et al. 2020). We use the quickstep framework within CP2K with the Gaussian and plane waves mixed bases (GPW). We adopt the Gaussian basis sets from VandeVondele et al. (2005); VandeVondele & Hutter (2007), in conjunction with the pseudopotentials (GTH-PBE) of Goedecker, Teter, and Hutter (Goedecker et al. 1996; Hartwigsen et al. 1998; Krack 2005).

Our system is converged for a planewave cutoff energy of 600 Ry and a REL_CUTOFF of 40 Ry. We use the revised PBE exchange functional GGA_X_PBE_R from Zhang & Yang (1998) and a PBE correlation functional, GGA_C_PBE (Perdew et al. 1996, 1997). These are found to be adequate choices when describing an aqueous system in conjunction with the non-local van der Waals correlation using the Grimme D3 method (Grimme et al. 2010), achieving convergence for R_CUTOFF of 14. The calculations were done done on a 2x2x2 supercell consisting of 32 CO molecules. The derived data at 0 K is obtained using CELL_OPT within CP2K and reported below.

4. THE EQUATION OF STATE

In table 1 and fig. 1 we give the volumes and energies derived for different pressures at 0 K. This data is fitted to a third order Birch-Murnaghan equation of state with a bulk modulus B= 6.556 ± 0.074 GPa, a pressure derivative for

Table 1. The volume, internal energy, and derived enthalpy as a function of pressure for the α-CO solid. Data is for a cubic supercell consisting of 32 CO molecules.

P [bar]	V [$\mathring{A}^3$]	U [Ha]	H [Ha]
30,000	1012.664	-694.3516	-693.6548
20,000	1063.250	-694.3819	-693.8941
10,000	1134.213	-694.4058	-694.1456
5000	1186.408	-694.4146	-694.2785
1000	1243.957	-694.4184	-694.3899
500	1252.903	-694.4185	-694.4041
250	1257.361	-694.4186	-694.4114
100	1260.298	-694.4186	-694.4157
50	1261.144	-694.4186	-694.4172
25	1261.663	-694.4186	-694.4179
10	1261.931	-694.4186	-694.4183
1	1262.103	-694.4186	-694.4186

the bulk modulus of $B' = 6.846 \pm 0.120$, and a zero pressure volume of $V_0 = 157.80 \pm 0.05\,\mathring{A}^3$. The error bars are at the 2σ level. As mentioned above, the QEOS requires a knowledge of ρ and B at reference conditions of zero energy, and, based on this calculation, and a fit to the four lowest pressure points we take $\rho = 1.179\,\mathrm{g\,cm^{-3}}$ and B$= 2.676\,\mathrm{GPa}$ as the input parameters. Note that this value of B falls between the best fit value of $6.556\,\mathrm{GPa}$ given above and the value of $1.3\,\mathrm{GPa}$ measured by Gammon (1978) for β-CO.

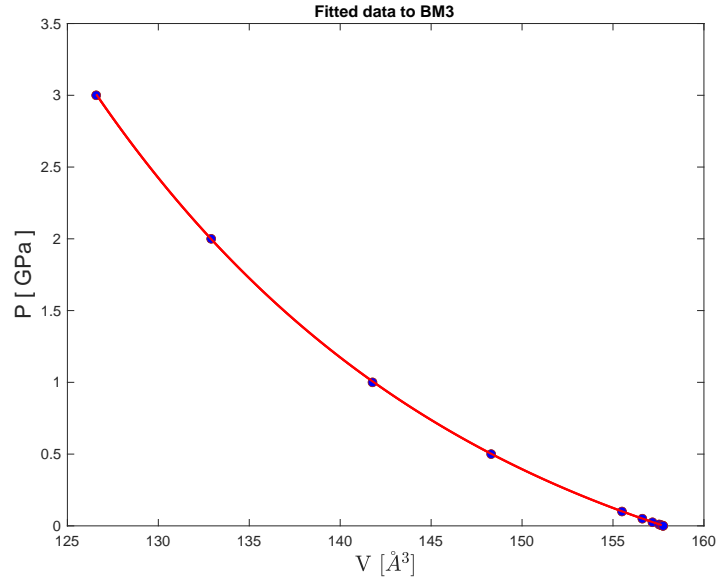**Figure 1.** Pressure versus unit cell volume for α-CO. The blue circles are unit cell volumes from our optimization data at $0\,\mathrm{K}$, and the solid red curve is the fitted third order Birch-Murnaghan equation of state (BM3).

Using the results of the DFT calculation described above in the quotidian code, we produced an equation of state

table giving the pressure, energy and entropy of CO for a large range of temperatures and densities.

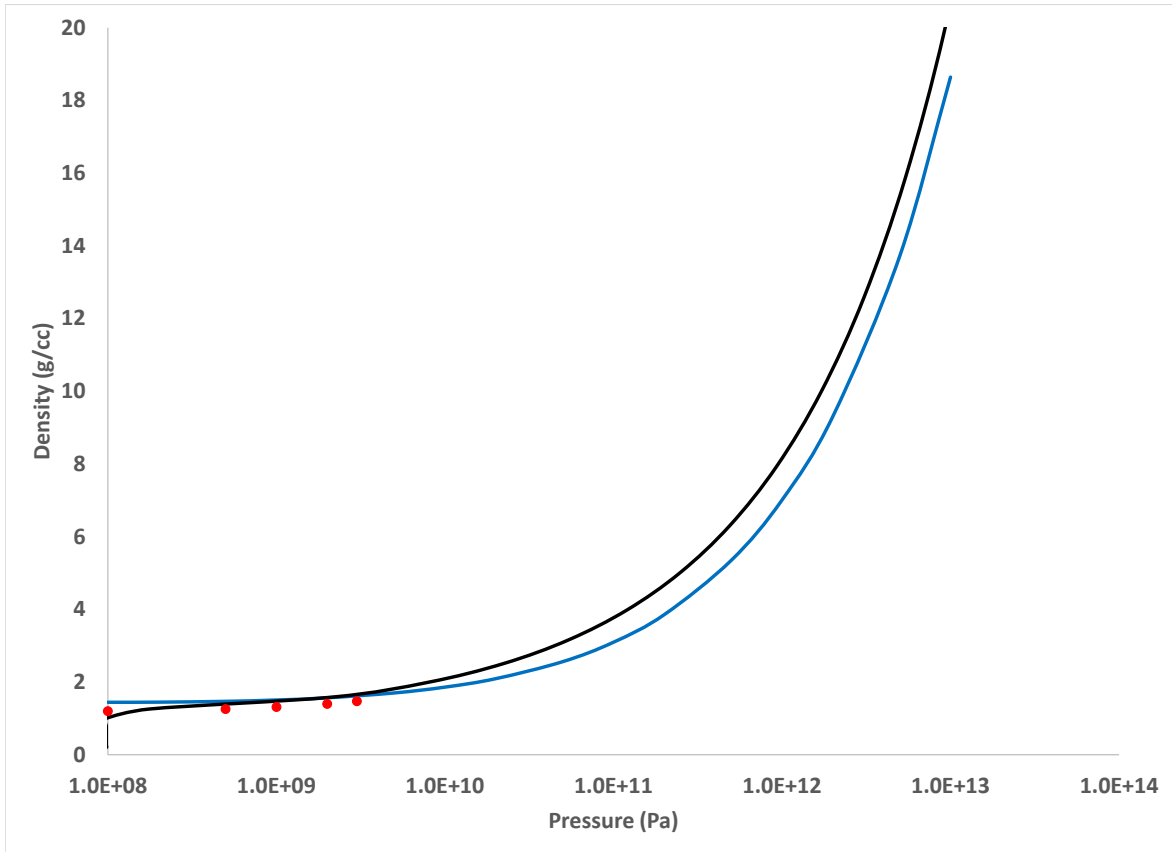## 5. COMPARISON TO OTHER RESULTS

Figure 2. Density as a function of pressure at zero temperature for the quotidian equation of state (black curve), and for the S-Z equation of state (blue curve). The red dots are the results of the DFT calculation.

Salpeter & Zapolsky (1967) (S-Z) describe a semi-empirical formula for predicting the zero temperature pressure-density relation for materials with any average atomic number. In principle, the S-Z EOS is similar to the More et al. (1988) approach, since it relies on a Thomas-Fermi-Dirac model of the atom. However it does not include the effect of temperature, so it is not always suitable for planet modeling. Fig. 2 shows the comparison between our quotidian equation of state (QEOS) at zero temperature, and the S-Z EOS. As can be seen, the agreement is excellent, and improves at higher pressures, as expected. The red dots in the figure are the DFT calculations given in table 1 and fig. 1. These fall right on the QEOS curve.

The QEOS can be compared to experimental data at higher temperatures as well. Goodwin (1985) gives the thermophysical properties of CO up to a pressure of $100\,\mathrm{MPa}$. Fig. 3 shows that data for an isotherm at $1000\,\mathrm{K}$ (red dots) compared to the QEOS isotherm at that temperature (black curve). The discontinuity in the QEOS is due to the fact that the QEOS finds two phases in present in this pressure-temperature range and traverses this region using a Maxwell construction. As a result, the computed pressure remains constant over the relevant density range. The actual pressure, as shown by the red dots, increases along the extrapolation of the lower part of the curve, as expected. The exact position of the phase transition is sensitive to the choice of input parameters (zero energy density and bulk modulus), and the actual value may be shifted somewhat.
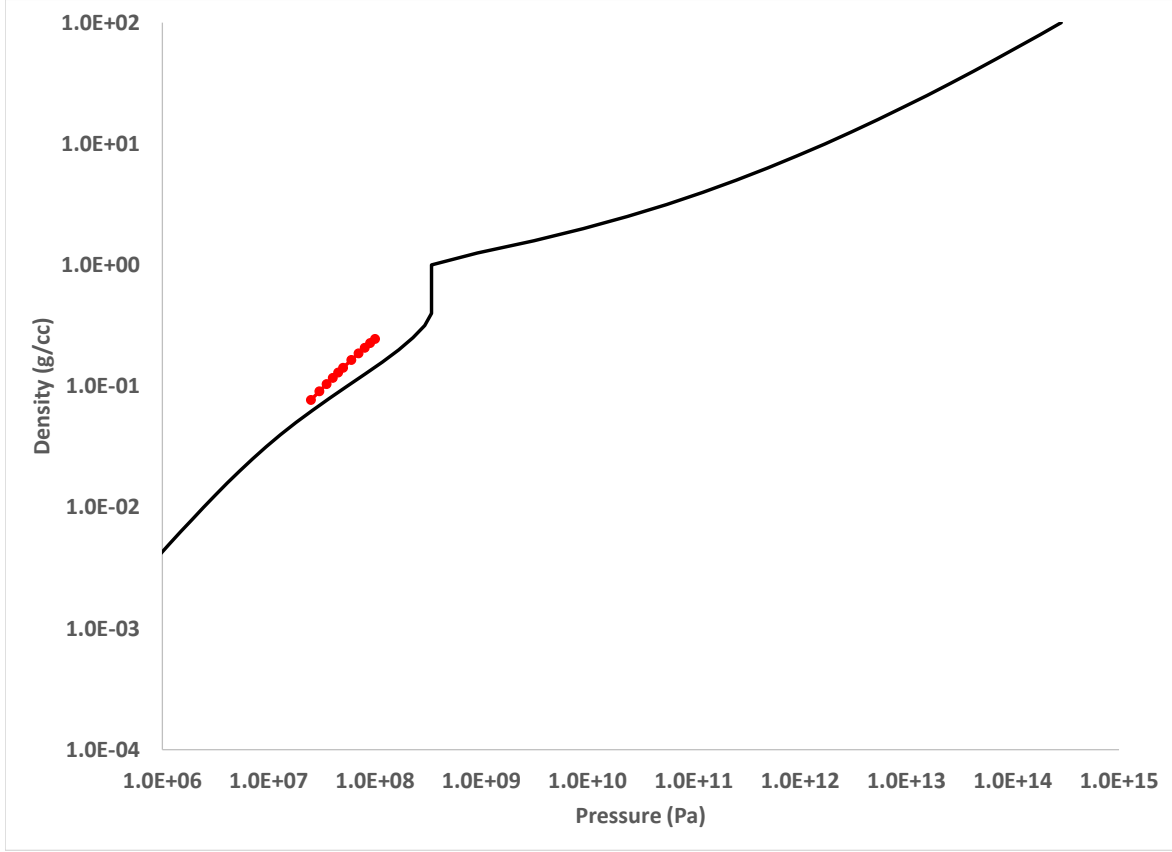
Figure 3. Density as a function of pressure for an isotherm at $T = 1000\,\mathrm{K}$ (black curve), compared to the data in Goodwin (1985) (red dots). See text for details.

At still higher pressures and temperatures, there are the shock wave experiments of Nellis et al. (1981). In this case the temperatures are only inferred from the Hugoniot relations, and are different for the different pressures. More recently, Zhang et al. (2011) have used quantum molecular dynamics calculations to compute points along a hugoniot. These are shown (blue dots) together with the hugoniot calculated from our QEOS in Fig. 4. The black dots are the experimental points of Nellis et al. (1981). As can be seen, the agreement is quite good and is in the range of these works. At the highest temperatures ($T \gtrsim 10^5\,\mathrm{K}$) dissociation and ionization become important, and these effects are not directly included in our calculation. Nonetheless, the energies we compute for CO at $T = 5 \times 10^5\,\mathrm{K}$ for densities of 0.1, 1, 10, and 100 $\mathrm{g\,cm^{-3}}$ all fall within a factor of 1.5 or less from the values shown in fig. 9 of Massacrier et al. (2011).

The full QEOS is summarized in Fig. 5. A short version for a range of pressures and temperatures that are expected to be important for planetary interior modeling given in table 2, while the complete table is available at the following site: CO EOS download.
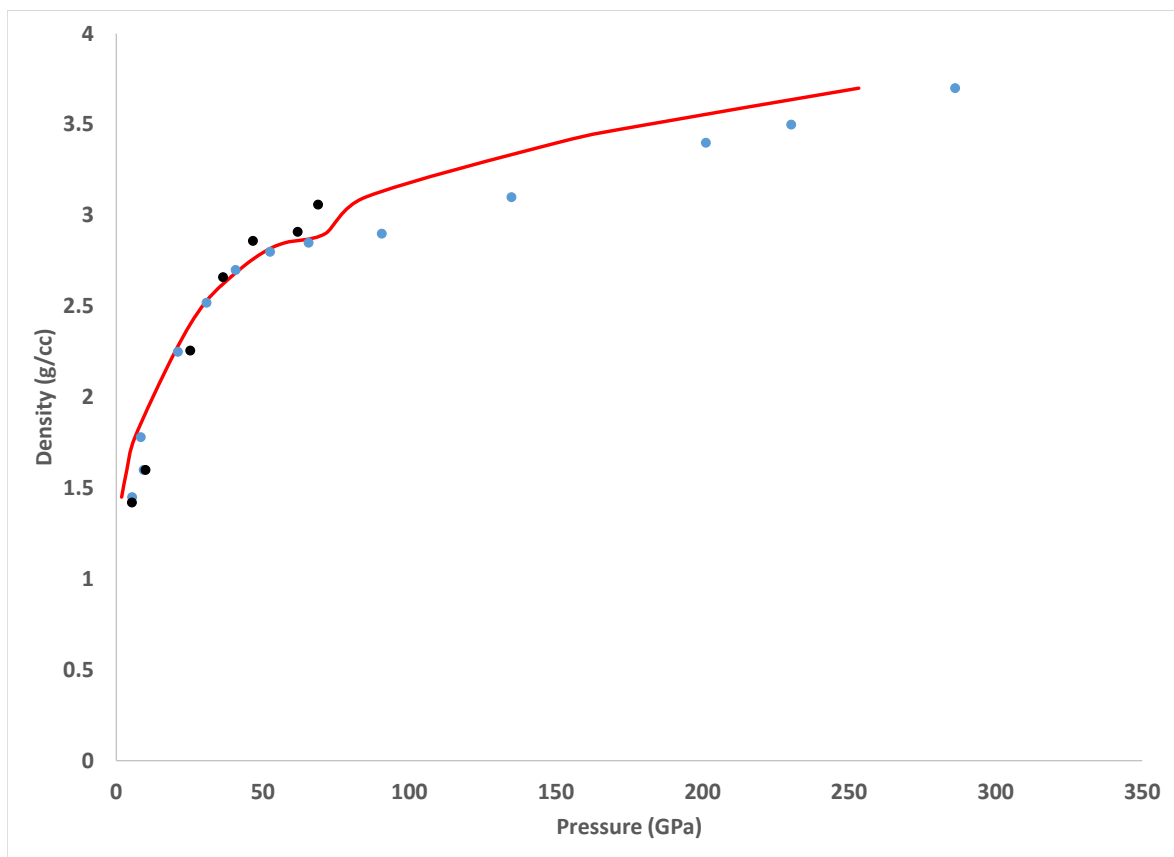
Figure 4. Density as a function of pressure for a hugoniot (blue curve) corresponding to the conditions of the shock experiments of Nellis et al. (1981) (black dots) and the quantum molecular dynamics calculations of Zhang et al. (2011) (blue dots).
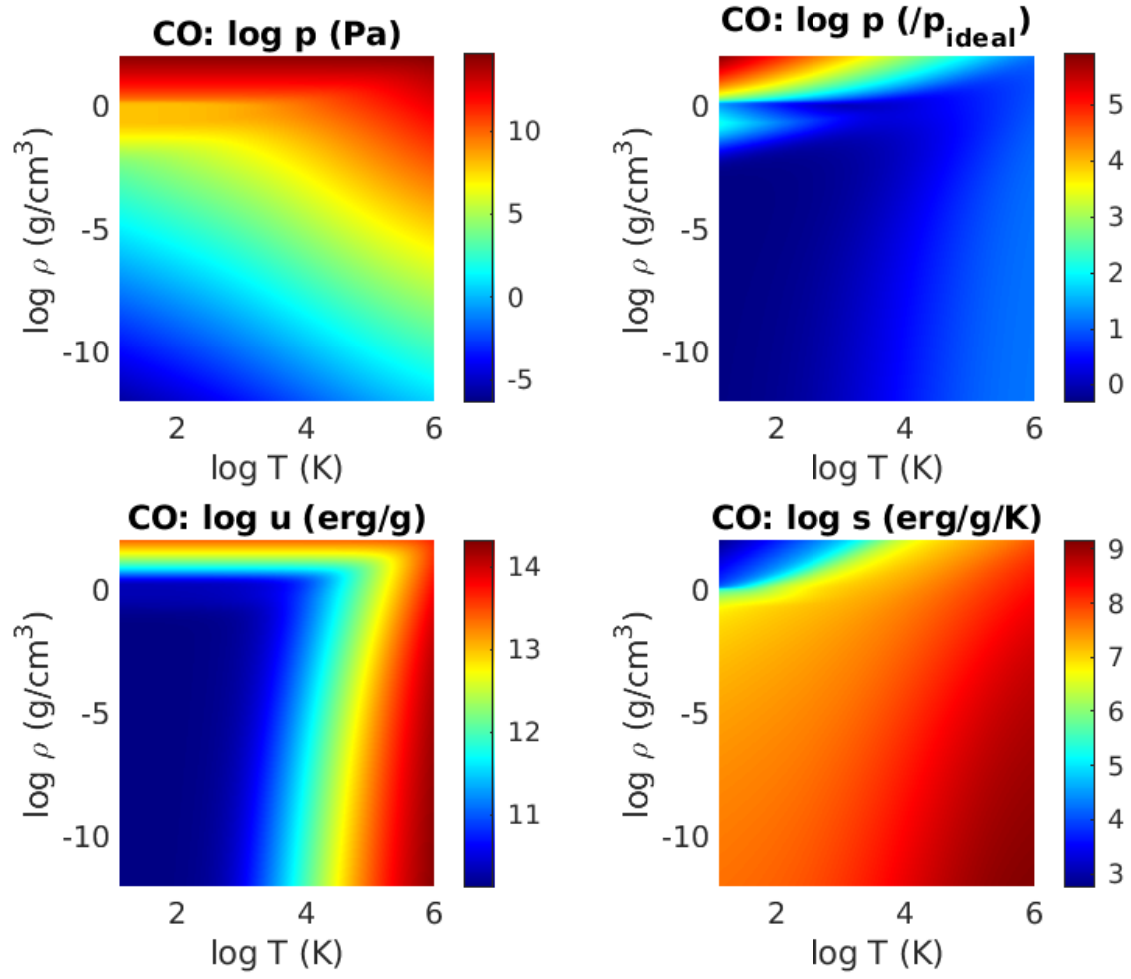
Figure 5. Thermodynamic properties of CO as a function of density and temperature as computed from the quotidian equation of state. **Upper left:** total pressure. **Upper right:** pressure divided by ideal gas pressure. This shows the region where an ideal gas approximation may be used. **Lower left:** specific internal energy. **Lower right:** specific entropy.

h

Table 2. Equation of state for CO.

$\log T$ [K]	$\log \rho$ [g/cc]	$\log P$ [Pa]	$\log u$ [erg/g]	$\log s$ [erg/g − K]
1.06465	0.10	8.25060	10.33294	4.12858
1.06465	0.20	9.33277	10.36235	3.94748
1.06465	0.30	9.90369	10.46041	3.83167
1.06465	0.40	10.35107	10.63593	3.74763
1.06465	0.50	10.73560	10.86075	3.67754
1.06465	0.60	11.08026	11.10070	3.61334
1.06465	0.70	11.39668	11.33587	3.55157
1.06465	0.80	11.69173	11.55846	3.49070
1.06465	0.90	11.96991	11.76663	3.43006
1.06465	1.00	12.23437	11.96089	3.36933
1.06465	1.10	12.48741	12.14250	3.30834
1.06465	1.20	12.73083	12.31285	3.24704
1.06465	1.30	12.96602	12.47327	3.18540
1.56465	0.10	8.25291	10.33305	5.29718
1.56465	0.20	9.33286	10.36239	4.92635
1.56465	0.30	9.90370	10.46043	4.63269
1.56465	0.40	10.35107	10.63594	4.42170
1.56465	0.50	10.73560	10.86075	4.27449
1.56465	0.60	11.08026	11.10070	4.16723
1.56465	0.70	11.39668	11.33587	4.08205
1.56465	0.80	11.69173	11.55846	4.00839
1.56465	0.90	11.96991	11.76663	3.94060
1.56465	1.00	12.23437	11.96089	3.87576
1.56465	1.10	12.48741	12.14250	3.81236
1.56465	1.20	12.73083	12.31285	3.74960
1.56465	1.30	12.96602	12.47327	3.68706
2.06465	0.10	8.32026	10.33617	6.33748
2.06465	0.20	9.33736	10.36427	6.10876
2.06465	0.30	9.90446	10.46124	5.82885
2.06465	0.40	10.35123	10.63621	5.53226
2.06465	0.50	10.73564	10.86083	5.24767
2.06465	0.60	11.08027	11.10073	5.00266
2.06465	0.70	11.39669	11.33588	4.80674
2.06465	0.80	11.69174	11.55846	4.65419
2.06465	0.90	11.96991	11.76663	4.53392
2.06465	1.00	12.23437	11.96089	4.43538
2.06465	1.10	12.48741	12.14250	4.35065
2.06465	1.20	12.73083	12.31285	4.27440
2.06465	1.30	12.96602	12.47327	4.20327
2.56465	0.10	8.59818	10.35536	6.81650
2.56465	0.20	9.37536	10.38058	6.71214
2.56465	0.30	9.91516	10.47251	6.59233
2.56465	0.40	10.35484	10.64227	6.45354
2.56465	0.50	10.73692	10.86349	6.29013

Table 2. Equation of state for CO continued

$\log T$ [K]	$\log \rho$ [g/cc]	$\log P$ [Pa]	$\log u$ [erg/g]	$\log s$ [erg/g − K]
2.56465	0.60	11.08076	11.10182	6.11803
2.56465	0.70	11.39686	11.33629	5.91384
2.56465	0.80	11.69180	11.55861	5.70071
2.56465	0.90	11.96994	11.76669	5.48884
2.56465	1.00	12.23438	11.96091	5.29094
2.56465	1.10	12.48742	12.14251	5.11592
2.56465	1.20	12.73083	12.31286	4.96608
2.56465	1.30	12.96602	12.47328	4.83886
3.06465	0.10	8.96463	10.41261	7.05238
3.06465	0.20	9.49348	10.43930	7.00870
3.06465	0.30	9.95968	10.52059	6.94781
3.06465	0.40	10.37374	10.67408	6.87899
3.06465	0.50	10.74579	10.88182	6.80456
3.06465	0.60	11.08515	11.11162	6.72332
3.06465	0.70	11.39912	11.34141	6.63379
3.06465	0.80	11.69298	11.56126	6.53419
3.06465	0.90	11.97055	11.76803	6.42218
3.06465	1.00	12.23471	11.96163	6.31293
3.06465	1.10	12.48758	12.14285	6.16560
3.06465	1.20	12.73092	12.31302	6.00969
3.06465	1.30	12.96606	12.47335	5.84475
3.56465	0.10	9.36962	10.57254	7.21587
3.56465	0.20	9.69405	10.59071	7.18659
3.56465	0.30	10.06369	10.65281	7.15510
3.56465	0.40	10.43076	10.77475	7.12114
3.56465	0.50	10.77783	10.94870	7.08214
3.56465	0.60	11.10251	11.15104	7.03402
3.56465	0.70	11.40902	11.36430	6.98398
3.56465	0.80	11.69886	11.57468	6.93149
3.56465	0.90	11.97416	11.77606	6.87593
3.56465	1.00	12.23696	11.96647	6.81651
3.56465	1.10	12.48903	12.14584	6.75230
3.56465	1.20	12.73184	12.31488	6.68219
3.56465	1.30	12.96665	12.47450	6.60487
4.06465	-1.00	8.72672	11.12752	7.61469
4.06465	-0.90	8.84338	11.11787	7.60037
4.06465	-0.80	8.96101	11.10873	7.58527
4.06465	-0.70	9.07819	11.09997	7.56926
4.06465	-0.60	9.19305	11.09161	7.55219
4.06465	-0.50	9.30353	11.08214	7.53390
4.06465	-0.40	9.40769	11.07207	7.51424
4.06465	-0.30	9.50433	11.06010	7.49310
4.06465	-0.20	9.59411	11.04556	7.47045
4.06465	-0.10	9.68161	11.02824	7.44633
4.06465	0.00	9.77804	11.00927	7.42091
4.06465	0.10	9.90243	10.99228	7.39448
4.06465	0.20	10.07443	10.98353	7.36684

Table 2. Equation of state for CO continued

$\log T$	$\log \rho$	$\log P$	$\log u$	$\log s$
$[K]$	$[g/cc]$	$[Pa]$	$[erg/g]$	$[erg/g - K]$
4.06465	0.30	10.30242	10.99646	7.33856
4.06465	0.40	10.57225	11.04588	7.30967
4.06465	0.50	10.86205	11.14146	7.28014
4.06465	0.60	11.15517	11.27981	7.24992
4.06465	0.70	11.44272	11.44692	7.21887
4.06465	0.80	11.72104	11.62736	7.18684
4.06465	0.90	11.98825	11.80866	7.14860
4.06465	1.00	12.24611	11.98690	7.10900
4.06465	1.10	12.49512	12.15893	7.06828
4.06465	1.20	12.73600	12.32343	7.02608
4.06465	1.30	12.96954	12.48020	6.98198
4.56465	-1.00	9.39391	11.85300	7.82194
4.56465	-0.90	9.49858	11.83884	7.80733
4.56465	-0.80	9.60479	11.82481	7.79226
4.56465	-0.70	9.71228	11.81091	7.77665
4.56465	-0.60	9.82054	11.79708	7.76038
4.56465	-0.50	9.92889	11.78321	7.74336
4.56465	-0.40	10.03655	11.76908	7.72545
4.56465	-0.30	10.14277	11.75438	7.70651
4.56465	-0.20	10.24707	11.73869	7.68639
4.56465	-0.10	10.34964	11.72211	7.66492
4.56465	0.00	10.45180	11.70292	7.64198
4.56465	0.10	10.55668	11.68314	7.61745
4.56465	0.20	10.66971	11.66302	7.59129
4.56465	0.30	10.79841	11.64539	7.56357
4.56465	0.40	10.95060	11.63526	7.53444
4.56465	0.50	11.13044	11.64026	7.50411
4.56465	0.60	11.33652	11.66954	7.47311
4.56465	0.70	11.56221	11.72900	7.44136
4.56465	0.80	11.79910	11.82012	7.40932
4.56465	0.90	12.04056	11.93746	7.37731
4.56465	1.00	12.28172	12.07201	7.34534
4.56465	1.10	12.51981	12.21535	7.31336
4.56465	1.20	12.75346	12.36132	7.28123
4.56465	1.30	12.98189	12.50572	7.24694
5.06465	-2.20	9.01221	12.79781	8.22267
5.06465	-2.10	9.10356	12.78341	8.20949
5.06465	-2.00	9.19496	12.76882	8.19617
5.06465	-1.90	9.28643	12.75405	8.18271
5.06465	-1.80	9.37804	12.73910	8.16910
5.06465	-1.70	9.46983	12.72399	8.15535
5.06465	-1.60	9.56187	12.70871	8.14144
5.06465	-1.50	9.65423	12.69328	8.12737
5.06465	-1.40	9.74698	12.67771	8.11312
5.06465	-1.30	9.84023	12.66200	8.09870
5.06465	-1.20	9.93407	12.64619	8.08407
5.06465	-1.10	10.02860	12.63027	8.06923

Table 2. Equation of state for CO continued

$\log T$	$\log \rho$	$\log P$	$\log u$	$\log s$
$[K]$	$[g/cc]$	$[Pa]$	$[erg/g]$	$[erg/g-K]$
5.06465	-1.00	10.12395	12.61427	8.05415
5.06465	-0.90	10.22023	12.59820	8.03880
5.06465	-0.80	10.31750	12.58210	8.02315
5.06465	-0.70	10.41581	12.56597	8.00716
5.06465	-0.60	10.51516	12.54983	7.99078
5.06465	-0.50	10.61545	12.53369	7.97396
5.06465	-0.40	10.71652	12.51752	7.95663
5.06465	-0.30	10.81818	12.50129	7.93872
5.06465	-0.20	10.92019	12.48494	7.92015
5.06465	-0.10	11.02242	12.46839	7.90082
5.06465	0.00	11.12490	12.45155	7.88063
5.06465	0.10	11.22793	12.43435	7.85947
5.06465	0.20	11.33226	12.41683	7.83721
5.06465	0.30	11.43918	12.39913	7.81373
5.06465	0.40	11.55056	12.38222	7.78890
5.06465	0.50	11.66886	12.36618	7.76260
5.06465	0.60	11.79684	12.35360	7.73472
5.06465	0.70	11.93708	12.34707	7.70521
5.06465	0.80	12.09132	12.35034	7.67410
5.06465	0.90	12.26000	12.36788	7.64155
5.06465	1.00	12.44186	12.40353	7.60770
5.06465	1.10	12.63451	12.45973	7.57309
5.06465	1.20	12.83475	12.53549	7.53795
5.06465	1.30	13.03937	12.62723	7.50218

6. ACKNOWLEDGEMENTS

REFERENCES

Armstrong, M. R., Lindsey, R. K., Goldman, N., et al. 2020, Nature Communications, 11, 353 1

Benz, W., Cameron, A. G. W., & Melosh, H. J. 1989, Icarus, 81, 113, doi: 10.1016/0019-1035(89)90129-2 1

Bierhals, J. 2001, in Ullmann's Encyclopedia of Industrial Chemistry, ed. F. Ullman (John Wiley & Sons, Ltd), doi: https://doi.org/10.1002/14356007.a05_203 1

Boon, J. P., Legros, J. C., & Thomaes, G. 1967, Physica, 33, 547, doi: 10.1016/0031-8914(67)90203-0 1

Chabrier, G., Mazevet, S., & Soubiran, F. 2019, ApJ, 872, 51, doi: 10.3847/1538-4357/aaf99f 1

Emsenhuber, A., Jutzi, M., & Benz, W. 2018, Icarus, 301, 247, doi: 10.1016/j.icarus.2017.09.017 1

Gammon, P. H. 1978, Master's thesis, Memorial University of Newfoundland 1, 4

Goedecker, S., Teter, M., & Hutter, J. 1996, Phys. Rev. B, 54, 1703, doi: 10.1103/PhysRevB.54.1703 3

Goodwin, R. D. 1985, Journal of Physical and Chemical Reference Data, 14, 849, doi: 10.1063/1.555742 1, 5, 3

Grimme, S., Antony, J., Ehrlich, S., & Krieg, H. 2010, The Journal of Chemical Physics, 132, 154104, doi: 10.1063/1.3382344 3

Haldemann, J., Alibert, Y., Mordasini, C., & Benz, W. 2020, A&A, 643, A105, doi: 10.1051/0004-6361/202038367 1

Hall, B. O., & James, H. M. 1976, Phys. Rev. B, 13, 3590, doi: 10.1103/PhysRevB.13.3590 3

Hartwigsen, C., Goedecker, S., & Hutter, J. 1998, Phys. Rev. B, 58, 3641, doi: 10.1103/PhysRevB.58.3641 3

Kühne, T. D., Iannuzzi, M., Del Ben, M., et al. 2020, The Journal of Chemical Physics, 152, 194103, doi: 10.1063/5.0007045 3

Krack, M. 2005, Theoretical Chemistry Accounts, 114, 145, doi: 10.1007/s00214-005-0655-y 3

Krüger, A., Kataoka, F., Ozawa, M., et al. 2005, Carbon, 43, 1722 1

Leonhardi, T. C., & Militzer, B. 2017, High Energy Density Physics, 22, 41, doi: https://doi.org/10.1016/j.hedp.2017.02.005 1

Lindsey, R. K., Goldman, N., Fried, L. E., & Bastea, S. 2020, J. Chem. Phys., 153, 054103 1

Lisse, C. M., Gladstone, G. R., Young, L. A., et al. 2022, The Planetary Science Journal, 3, 112, doi: 10.3847/PSJ/ac6097 1

Massacrier, G., Potekhin, A., & Chabrier, G. 2011, Phys. Rev. E, 84, doi: 10.1103/PhysRevE.84.056406 1, 5

Melosh, H. J. 2007, Meteoritics and Planetary Science, 42, 2079, doi: 10.1111/j.1945-5100.2007.tb01009.x 1

More, R. M., Warren, D. A., Young, D. A., & Zimmerman, G. B. 1988, Physics of Fluids, 31, 3059 (document), 2, 5

Nellis, W. J., Ree, F. H., van Thiel, M., & Mitchell, A. C. 1981, J. Chem. Phys., 75, 3055, doi: 10.1063/1.442401 1, 5, 4

Perdew, J. P., Burke, K., & Ernzerhof, M. 1996, Phys. Rev. Lett., 77, 3865, doi: 10.1103/PhysRevLett.77.3865 3

—. 1997, Phys. Rev. Lett., 78, 1396, doi: 10.1103/PhysRevLett.78.1396 3

Pierazzo, E., Artemieva, N., & Ivanov, B. 2005, in Large Meteorite Impacts III (Geological Society of America), doi: 10.1130/0-8137-2384-1.443 1

Pierazzo, E., Vickery, A. M., & Melosh, H. J. 1997, Icarus, 127, 408, doi: 10.1006/icar.1997.5713 1

Podolak, J., Malamud, U., & Podolak, M. 2022, Icarus, 382, doi: 10.1016/j.icarus.2022.115017 1

Rudesko, N. S., & Schubnikow, L. W. 1934, Phys. Z. Sowjet., 6, 470 1

Salpeter, E. E., & Zapolsky, H. S. 1967, Phys. Rev., 158, 876, doi: 10.1103/PhysRev.158.876 5

Singraber, A., Behler, J., & Dellago, C. 2019, J. Chem. Theory Comput., 15, 1827 1

Tancredi, G., Rickman, H., & Greenberg, J. M. 1994, Astronomy and Astrophysics, 286, 659 1

Titov, V. M., Anisichkin, V. F., & Mal'kov, I. Y. 1989, Combust. Explos. Shock Waves, 25, 372 1

VandeVondele, J., & Hutter, J. 2007, The Journal of Chemical Physics, 127, 114105, doi: 10.1063/1.2770708 3

VandeVondele, J., Krack, M., Mohamed, F., et al. 2005, Computer Physics Communications, 167, 103 , doi: https://doi.org/10.1016/j.cpc.2004.12.014 3

Vazan, A., Kovetz, A., Podolak, M., & Helled, R. 2013, MNRAS, 434, 3283, doi: 10.1093/mnras/stt1248 2

Vazan, A., Ormel, C. W., Noack, L., & Dominik, C. 2018, ApJ, 869, 163, doi: 10.3847/1538-4357/aaef33 2

Vazan, A., Sari, R., & Kessel, R. 2022, ApJ, 926, 150, doi: 10.3847/1538-4357/ac458c 2

Viecelli, J. A., Bastea, S., Glosli, J. N., & Ree, F. H. 2001, J. Chem. Phys., 115, 2730 1

Wang, C., & Zhang, P. 2010, J. Chem. Phys., 133, doi: 10.1063/1.3491834 1

Zhang, Y., Wang, C., Li, D., & Zhang, P. 2011, J. Chem. Phys., 135, doi: 10.1063/1.3624920 1, 5, 4

Zhang, Y., & Yang, W. 1998, Phys. Rev. Lett., 80, 890, doi: 10.1103/PhysRevLett.80.890 3